Published in final edited form as:
Dev Dyn. 2014 November ; 243(11): 1457–1469. doi:10.1002/dvdy.24168.

Role of *semaphorin-1a* in the developing visual system of the disease vector mosquito *Aedes aegypti*

Keshava Mysore[1,2], **Ellen Flannery**[2,3], **Matthew T. Leming**[2,3], **Michael Tomchaney**[2,3], **Lucy Shi**[2,3], **Longhua Sun**[2,3], **Joseph E. O'Tousa**[2,3], **David W. Severson**[1,2,3], and **Molly Duman-Scheel**[1,2,3,4]

[1]Department of Medical and Molecular Genetics, Indiana University School of Medicine, Raclin-Carmichael Hall, South Bend, Indiana, 46617, USA

[2]Eck Institute for Global Health, Brownson Hall, University of Notre Dame, Notre Dame, Indiana, 46556, USA

[3]Department of Biological Sciences, Galvin Life Sciences, University of Notre Dame, Notre Dame, Indiana, 46556, USA

Abstract

Background—Despite the devastating impact of mosquito-borne illnesses on human health, very little is known about mosquito developmental biology, including development of the mosquito visual system. Mosquitoes possess functional adult compound eyes as larvae, a trait that makes them an interesting model in which to study comparative developmental genetics. Here, we functionally characterize visual system development in the dengue and yellow fever vector mosquito *Aedes aegypti,* in which we use chitosan/siRNA nanoparticles to target the axon guidance gene *semaphorin-1a (sema1a)*.

Results—Immunohistochemical analyses revealed the progression of visual sensory neuron targeting that results in generation of the retinotopic map in the mosquito optic lobe. Loss of *sema1a* function led to optic lobe phenotypes, including defective targeting of visual sensory and higher order neurons and failed formation of the retinotopic map. These *sema1a* knockdown phenotypes correlated with larval photoavoidance behavioral defects.

Conclusions—The results of this investigation indicate that Sema1a is required for optic lobe development in *A. aegypti* and highlight the behavioral importance of a functioning visual system in pre-adult mosquitoes.

Keywords

Semaphorin; *Aedes aegypti*; vision; eye; development; mosquito; siRNA; nanoparticle; sensory system; optic lobe; targeting

[4]To whom correspondence should be addressed mscheel@nd.edu Indiana University School of Medicine Raclin-Carmichael Hall 1234 Notre Dame Ave. South Bend, IN 46617 Phone: (574) 631-7194 Fax: (574) 631-7821 .

COMPETING INTERESTS: The authors declare that they have no competing interests.

AUTHORS' CONTRIBUTIONS: Conceived and designed the experiments: KM, EF, ML, MDS. Performed the experiments: KM, EF, ML, LuS, LoS, MT. Analyzed the data: KM, EF, ML, MT, JO, DWS, MDS. Contributed reagents and analysis tools: ML and JO. Prepared the manuscript: KM, EF, ML, JO, DWS, and MDS.

INTRODUCTION

In insects, visual perception of environmental cues plays a key role in a variety of behavioral outputs at multiple stages of the life cycle. Vision is often integrated with other senses, mainly olfaction, to permit mating, the location of food sources and oviposition sites, and in hematophagous mosquitoes, identification of blood meal hosts (Allan et al., 1987; Bentley and Day, 1989; Bowen, 1991). Knowledge of the development, structure, and central processing of sensory modalities would greatly improve our understanding of complex behaviors in mosquitoes. In an effort to address this, we are investigating the development of sensory systems in *Aedes aegypti*, the dengue and yellow fever vector mosquito (Clemons et al., 2010a; Mysore et al., 2011; Mysore et al., 2013; Mysore et al., 2014). Here, we functionally characterize development of the *A. aegypti* visual system. Although research is generating an understanding of how visual inputs contribute to adult mosquito behavior (reviewed by Allan et al., 1987; Bentley and Day, 1989; Bowen, 1991), development of the mosquito visual system and its role in developing mosquitoes is not well understood.

To date, development of the insect visual system has been most extensively studied in the fruit fly *Drosophila melanogaster* (Moses, 2002), which possesses one of the most derived modes of insect eye development. The fruit fly larval visual system consists of three photosensory ocelli and a set of simple larval eyes, the Bolwig organs. The *Drosophila* eye imaginal disc, which gives rise to the adult retina, initiates differentiation during the third larval instar. The retina undergoes extensive transformation toward adult morphology during the resting pupal stage, after which time it becomes fully functional. Like *Drosophila,* the visual system of most holometabolous insects transforms into the adult visual system during the pupal resting phase (Friedrich, 2003). Although mosquitoes are holometabolous insects, adult eye cells have been identified on the basis of morphological characters in larvae, and these eyes are believed to be functional during the late larval and pupal stages (Gilbert, 1994; Buschbeck and Friedrich, 2008). Thus, mosquitoes an interesting model in which to study the neural and evolutionary basis of insect visual system development.

In the present study, we characterize the progression of post-embryonic visual system development and functionally assess the visual sensory neuron targeting process responsible for generation of the retinotopic map in the *A. aegypti* optic lobe. We then examine the role of *A. aegypti* Semaphorin-1a *(Aae* Sema1a) during larval and pupal optic lobe development. *Aae* Sema1a belongs to the Sema family of axon guidance molecules (Haugen et al., 2011) that are well known for their roles in the regulation of nervous system development in a variety of organisms (Flannery and Duman-Scheel, 2009). Previous studies from our laboratory revealed that Sema1a is required during mosquito embryonic nerve cord development (Haugen et al., 2011), while a recent report (Mysore et al., 2013) describes its role during *A. aegypti* olfactory system development. In the developing *D. melanogaster* visual system, Sema1a is required in pre-adult photoreceptor (R-cell) axons to establish the appropriate topographic termination pattern in the optic lobe of the brain (Cafferty et al., 2006). Sema1a also regulates targeting of the *Drosophila* L3 lamina neuron growth cones, which extend from the lamina into the M3 medulla neuropil layer during the pupal stage

(Pecot et al., 2013). Based on our observation that Sema1a is expressed in the developing *A. aegypti* visual system, we hypothesize that it regulates formation of the retinotopic map in the mosquito optic lobe. However, given the differences in *D. melanogaster* and *A. aegypti* adult visual system development noted above, the precise roles of this axon guidance molecule may differ during visual system development in the two species. Here, we examine the role of Sema1a in the developing *A. aegypti* larval and pupal visual system through the application of various cross reacting antibodies (Mysore et al., 2011; Mysore et al., 2013) and through use of the chitosan/siRNA gene targeting technique recently optimized in *A. aegypti* (Mysore et al., 2013; Mysore et al., 2014). These studies revealed that *sema1a* function is required for development of the visual system and for processing of visual sensory information in *A. aegypti* larvae.

RESULTS AND DISCUSSION

Visual system development in A. aegypti

The *A. aegypti* larval eye is present during the L1-L4 larval stages and persists at least through 48 h after pupal formation (APF; Fig. 1). The larval eye is composed of lateral ocelli (White, 1961; Brown and White, 1972) that possess rhodopsin, respond to visual stimuli (Brown and White, 1972; Seldin et al., 1972), and contribute to development of the adult compound eye, which can first be observed in L3 larvae (Fig. 1C). In *D. melanogaster,* the adult eye is derived from the eye-antennal disc, which forms during head involution when presumptive eye-antennal tissue in the dorsolateral ectoderm folds internally (reviewed by Wolff and Ready, 1993). Unlike *D. melanogaster, A. aegypti* does not possess an eye imaginal disc, which is not an obligate feature of retinal development in all holometabolous insects (Friedrich, 2003). Instead, the adult eye develops in the eye placode region of the larval head, the future retinal field of the adult head capsule (White, 1961), with rows of photoreceptor cell clusters being added over time (Fig. 1D-F). This mode of eye development is reminiscent of *Tribolium castaneum* eye development, except that the mosquito adult eye is believed to be functional in late larval and pupal stages (Gilbert, 1994; Buschbeck and Friedrich, 2008), whereas much like *Drosophila*, terminal differentiation of the *Tribolium castaneum* eye does not initiate until the resting pupal stage (Friedrich, 2003). In contrast, hemimetabolous insects like grasshoppers and cockroaches are born with adult-like eyes that are functional in first instar nymphs, grow between subsequent molts, and are maintained in adults (Friedrich, 2003). Although other holometabolous insects, including the tiger beetle *Cicindela chinensis,* have a specialized larval visual system for predation (Toh and Mizutani, 1987), the presence of functioning adult compound eyes during the larval stages has not to our knowledge been reported in other holometabolous insect species.

Progressive development of the larval and adult eyes and corresponding development of the brain was tracked from stage L1 (Fig. 2A1-A3) through 48h APF (Fig. 2F1-F3). mAb 22C10 (Fig. 2A1-F1), a marker for visual sensory neurons (Fujita et al., 1982; Zipursky et al., 1984), was found to co-label with anti-acetylated tubulin antibody staining (Fig. 2A2-F2), which was used to label the visual sensory neurons throughout the rest of the investigation. During stage L1, axons from the larval eye target to the developing brain through the developing primary visual center (Fig. 2A1-A3), which cannot be differentiated

into various neuropiles at this stage. By stage L3 (Fig. 2C1-C3), axons from the developing adult eye are also visible. Visual sensory neurons from both the larval and adult eyes project together to the optic lobe of the brain (Fig. 2C3-F3). By the pupal stages, a complex visual center has formed (Fig. 2E1-E3, F1-F3).

Sema1a is required for proper targeting and sorting of visual sensory neurons during development

Sema1a protein expression is observed in fourth instar visual sensory neurons (Fig. 3A2), as well as in the L4 optic lobe to which Sema1a-positive visual sensory neurons target (Fig. 3A2; see also *sema1a* transcripts in the optic lobe in Fig. 3A1). Expression of Sema1a protein is maintained in 24 h pupae (the midpoint of pupal development), at which time Sema1a is expressed throughout the entire optic lobe (Fig. 3E2; see also Fig. 3E1 for *sema1a* transcript expression). Note that the specificity of the anti-Sema1a antibody used in these assays was confirmed in previous studies (Mysore et al., 2013), and again here through *sema1a* knockdown (KD) experiments in which staining with this reagent was absent (Fig. 3, see below). The Sema1a expression patterns in the developing *A. aegypti* visual system are similar to those described in *D. melanogaster* (Cafferty et al., 2006), in which Sema1a staining is observed in photoreceptor neurons and the lamina of the optic lobe.

In an effort to understand the putative role of *sema1a* during *A. aegypti* visual development, the chitosan/siRNA larval feeding method (Mysore et al., 2013) was used for delivery of control siRNA (Haugen et al., 2011) or two different *sema1a* KD siRNAs (siRNA^{890} and siRNA^{1198}) which have been used to target *sema1a* in previous investigations (Haugen et al., 2011; Mysore et al., 2013). Following *sema1a* KD siRNA^{890} or siRNA^{1198} feedings, *in situ* hybridization and anti-Sema1a antibody staining assays revealed KD of *sema1a* in the developing visual system in both L4 larvae (Fig. 3C1, C2, D1, D2 vs. A1, A2, B1, B2, Table 1) and 24 h pupae (Fig. 3G1, G2, H1, H2 vs. E1, E2, F1, F2, Table 1), which correspond to the stages in which morphological and behavioral phenotypes were analyzed in this investigation. Similar to Mysore et al. (2013), *in situ* hybridization assays revealed reduced *sema1a* levels in ~75% of L4 larvae and ~64% of 24 h pupae (Table 1). These assays failed to detect *sema1a* transcript or Sema1a protein in a subset (roughly one-third of the visual systems analyzed, n=50 larvae and 50 pupae per siRNA treatment) of *sema1a* KD animals (Fig. 3C1, C2, D1, D2, G1, G2, H1, H2). As in the previous investigation (Mysore et al., 2013), all phenotypes (Table 2) were scored in such individuals, which were identified on the basis of a lack of detectable Sema1a expression as ascertained through anti-Sema1a staining. All KD phenotypes reported herein were observed in both siRNA^{890} and siRNA^{1198} animals (Table 2), which helped to ensure that the phenotypes generated were not simply the result of off-site targeting by either siRNA. None of the loss of function phenotypes described herein were observed in control-fed animals (Table 2), which were comparable to wildtype animals for all phenotypes assessed.

In wildtype (Fig. 4A1-A3) and control-fed (Fig. 4B1-B3) individuals, fourth instar visual sensory neurons labeled by anti-Sema1a antibody and anti-acetylated Tubulin antibody staining send axons toward the posterior end of the brain where they converge and enter the optic stalk and then project to the lamina. Within the lamina, a majority of these axons

condense and form a dense terminal layer, the lamina plexus, while a subset of the growth cones pass through the lamina into the medulla and generate a topographic termination pattern (Figs. 4A1-A3, B1-B3). These sensory neurons form a retinotopic map of visual sensory neurons that has the same pattern in all wildtype (Fig. 4A1-A3) and control-fed (Fig. 4B1-B3) individuals. Although we lack the tools for distinguishing specific photoreceptor types that are available in *Drosophila*, the retinotopic map formed in *A. aegypti* L4 larvae bears strong resemblance to that which has been described in third instar *D. melanogaster* larvae (reviewed in Paulk et al., 2013).

In L4 larvae fed with *sema1a* KD siRNA^{890} (Fig. 4C1-C3) or siRNA^{1198} (Fig. 4D1-D3), visual sensory neurons enter and exit the optic stalk normally, progressing to the optic lobe of the brain as a bundle. However, within the lamina, visual sensory neurons fail to sort into the retinotopic pattern observed in wildtype and control individuals (Fig. 4C1-C3, D1-D3 vs. A1-A3, B1-B3, Table 2). A proper terminal layer does not form; many visual sensory neurons collapse together near the location where the terminal layer would normally form and then project together to the medulla, where they fail to generate proper topographic termination patterns (Fig. 4C1-3, D1-D3). These targeting phenotypes do not appear to be secondary to general R-cell differentiation defects, as no obvious defects in rhadomere structure were observed following *sema1a* KD (Fig. 3E3-H3). Moreover, full-field adult electroretinogram (ERG) analyses indicated that R-cells in *sema1a* KD animals respond to light appropriately (Fig. 5A, B).

These siRNA-mediated gene targeting experiments (Fig. 4) demonstrated that *A. aegypti* Sema1a, like *D. melanogaster* Sema1a (Cafferty et al., 2006), is required for establishment of the retinotopic map in the optic lobe. In both insects, loss of *sema1a* results in disrupted formation of the lamina plexus. However, although defects in R-cell axon termination patterns were detected in *Drosophila sema1a* loss of function homozygous animals, lamina vs. medulla target selection was essentially normal in these animals. This is not the case in *A. aegypti sema1a* loss of function animals generated through siRNA-mediated KD, in which many visual sensory axons project beyond the lamina into the medulla (Fig. 4C1-3, D1-3). Similarly, we also previously reported differences in the *A. aegypti* and *D. melanogaster sema1a* loss of function embryonic nerve cord phenotypes (Haugen et al., 2011).

In *Drosophila,* Sema1a, a transmembrane molecule, functions as a receptor for Plexin (Plex) ligands. However, Sema1a can also function as a ligand for Plexin receptors during neural development (reviewed by Flannery and Duman-Scheel, 2009). In the developing *D. melanogaster* visual system, in which this phenomenon was initially reported, Sema1a is a ligand for the PlexA receptor (Cafferty et al., 2006; Yu et al., 2010). Sema1a-PlexA forward signaling mediates axon-axon repulsion during *Drosophila* motor axon guidance (Winberg et al., 1998; Yu et al.,1998). However, Yu et al. (2010) postulated that Sema1a-PlexA reverse signaling mediates attractive axon-axon interactions for the proper organization of R-cell growth cones in the terminal layer. Thus, Sema1a could function as a ligand or receptor in the developing *A. aegypti* visual system. And given that it is expressed in both the visual sensory neurons and their optic lobe target (Figs. 3A1, A2, 4A1), it could conceivably function in either or both locations during visual development. The

development of more sophisticated genetic analysis tools in *A. aegypti* would permit investigation of these questions, as well as analysis of whether Sema1a signaling plays an attractive or repulsive role during visual sensory neuron targeting in *A. aegypti*.

Sema1a is required for light avoidance behavior

Given the visual sensory neural targeting defects observed in *sema1a* KD animals (Fig. 4C1-3; D1-D3), it was hypothesized that these larvae may have altered behavioral responses to light cues. *A. aegypti* larvae exhibit photoavoidance behavior (reviewed in Christophers, 1960), a response that can be measured in a simple behavioral assay (see methods for details; n = 25 animals in each control or experimental group in all four replicate experiments, Fig. 6). Wildtype and control-fed L4 individuals respond to light by moving to the darkest available zone of a petri dish within 5 sec of light introduction (Fig. 6A, B). Upon reaching the dark, wildtype and control-fed animals remained in the 100% darkness zone for the duration of the 60 s assay (Fig. 6A, C, D). No significant differences were detected between wildtype and control-fed animals in these behavioral assays ($p>0.9$; Fig. 6B-D). *sema1a* KD animals fed with siRNA^{890} or siRNA^{1198} also move toward darkness (Fig. 6A), but at a significantly slower rate than wildtype or control fed-animals (2x slower; $p<0.001$; Fig. 6B). In comparison to wildtype and control-fed animals, *sema1a* KD animals fed with either siRNA^{890} or siRNA^{1198} remained in 100% darkness (Fig. 6A) for a significantly shorter period of time ($p<0.001$; Fig. 6C). At the end of the assay (Fig. 6A), in comparison to wildtype and control-fed larvae, all of which were found in the 100% darkness zone, a significantly lower percentage of *sema1a* KD larvae fed with siRNA^{890} (61%) or siRNA^{1198} (58%) remained in the darkest zone ($p<0.001$; Fig. 6D). No significant differences were detected between animals fed with siRNA^{890} or siRNA^{1198} in these assays ($p>0.5$; Fig. 6B-D). These results suggest that loss of *sema1a* slows L4 larvae's initial response to light and impedes their prolonged light avoidance behavior.

Given that full-field ERG assays did not detect decreased light sensitivity in R-cells of *sema1a* KD animals (Fig. 5A, B), dysfunctional higher order processing of light sensory cues could be responsible for the altered light avoidance behavior detected in these individuals (Fig. 6). In light of the visual sensory neuron targeting defects observed (Fig. 4), it was hypothesized that *sema1a* KD may disrupt higher order neurons that relay visual information to higher brain centers. Although there is almost no data available regarding the detailed organization of the visual system in *A. aegypti* mosquitoes, a previous study by Mysore et al. (2011) indicated that a subset of these higher order neurons in the optic lobe are labeled by anti-serotonin (5HT) antibody. We used this reagent to pursue more detailed analysis of the *A. aegypti* developing visual system. Anti-5HT staining of wildtype (Fig. 7A1-3) and control-fed (Fig. 7B1-3) L4 larvae revealed a set of higher order neurons that originate in the supraoesophageal ganglion, pass through the medulla, and eventually terminate in the lamina, the region where the primary visual sensory neurons initially sort to form a retinotopic map (Fig. 7A1, B1). By the pupal stage, 5HT-positive higher order neurons originating in the supraoesophageal ganglion have sent extensive projections to the lobula in wildtype (Fig. 8A1-3) and control-fed (Fig. 8B1-3) animals. In *sema1a* KD L4 individuals fed with either siRNA^{890} (Fig. 7C1-3) or siRNA^{1198} (Fig. 7D1-3), 5HT-positive higher order neurons can be detected in the supraoesophageal ganglion and occasionally

enter the medulla, but terminate early and fail to reach their laminar targets (Fig. 7C1, D1; Table 2). These phenotypes correspond with decreased Sema1a expression (Fig. 7C2, D2; compare to Sema1a levels in wildtype and control-fed animals in Fig. 7A2, B2; overlays are shown in Fig. 7A3-D3). In 24h APF *sema1a* KD pupae fed with either KD siRNA^{890} (Fig. 8C1-3) or siRNA^{1198} (Fig. 8D1-3), these projections terminate before entering the lobula (Fig. 8C1, D1; Table 2). This phenotype corresponds with decreased Sema1a levels (Fig. 8C2, D2; compare to Sema1a levels in wildtype and control-fed animals in Fig. 8A2, B2; overlays are shown in Fig. 8A3-D3). These findings suggest that loss of *sema1a* disrupts targeting of neurons that relay visual information to higher brain centers. It is presently unclear if Sema1a function is required in the higher order neurons or in the lobula, to which they target.

The visual sensory and higher order neural defects observed in *sema1a* KD animals (Figs. 4, 7, Table 2) suggest that their lack of prolonged light avoidance behavior (Fig. 6A, C, D) results from dysfunctional higher order visual processing. Given the significant defects detected in the optic lobes of *sema1a* KD animals (Figs. 4, 7), one might have anticipated that these larvae would not respond to light at all. However, *sema1a* animals do initially exhibit light avoidance behavior, albeit at a slower rate than their wildtype and control-fed counterparts (Fig. 6A, B). These animals had no noticeable motor defects that impeded their ability to move toward darkness, as evidenced by their increased ability to move away from it (Fig. 6C). Extra-ocular body wall photoreceptors can mediate light avoidance behavior in *D. melanogaster,* even when the larval eye is ablated (Xiang et al., 2010). It is not presently known whether *A. aegypti* possess class IV dendritic arborization neurons that function as body wall photoreceptors (Xiang et al., 2010), but the dendrites of these neurons are known to tile the body wall in other insects (Grueber et al., 2001), and *A. aegypti* possesses orthologs of Gr28b and TrpA1 (Megy et al., 2012), both of which have been implicated in *D. melanogaster* class IV dendritic neural phototransduction (Xiang et al., 2010). Furthermore, although *Aae sema1a* KD larvae initially exhibit photoavoidance behavior, this response to light is delayed, which is interesting given that extra-ocular photoreceptors typically have longer reaction times in comparison to ocular photoreceptors (Steven, 1963).

The results of this investigation indicate that loss of Sema1a function during *A. aegypti* visual system development results in optic lobe defects, including defective targeting of visual sensory neurons and failed formation of the retinotopic map (Fig. 4), as well as higher order visual neuron defects (Figs. 7, 8). In addition to significant differences in the formation of the *D. melanogaster* and *A. aegypti* visual systems (Fig. 1; Buschbeck and Friedrich, 2008), the *sema1a* loss of function visual sensory neuron targeting phenotypes observed in *A. aegypti* (Fig. 4) differ from those described in the fruit fly (Cafferty et al., 2006). In short, although the lamina vs. medulla target selection decision remains in tact in most *D. melanogaster* homozygous *sema1a* mutant animals, it is disrupted in *A. aegypti sema1a* KD animals. It will be useful to develop tools for manipulation of gene expression in select tissues or neurons in *A. aegypti,* which would allow for determination of whether Sema1a reverse signaling mediates attraction in visual sensory neurons, as has been suggested in *D. melanogaster* (Cafferty et al., 2006; Yu et al., 2010), or if Sema1a signaling mediates repulsion in *A. aegypti* visual sensory neurons. It will also be interesting to determine if higher order serotonergic visual system neurons are disrupted in *D.*

melanogaster sema1a loss of function mutants as they are in *A. aegypti* (Figs. 7, 8). Furthermore, L3 neural growth cone targeting in the *Drosophila* pupal medulla requires Sema1a signaling (Pecot et al., 2013), and so it would be good to determine if this is the case in *A. aegypti*. Unfortunately, we presently lack specific markers for these neurons, as well as the many other neurons in the mosquito visual medulla neuropil that could potentially be impacted by loss of Sema1a signaling. Identification of molecular markers for additional cellular components of the *A. aegypti* visual system will help us to address these issues in the future. Finally, the optic lobe defects that were observed in *A. aegypti sema1a* KD animals in this investigation (Figs. 4, 7) correlated with larval photoavoidance behavioral phenotypes, including a delayed initial response to light and disruption of prolonged light avoidance behavior (Fig. 6). These *sema1a* loss of function photoavoidance defects underscore the importance of the visual sensory system in mosquito larvae, which presumably utilize this behavior to escape to shadows in which they can hide from predators that are better able to see them in the light.

EXPERIMENTAL PROCEDURES

Mosquito rearing

The *A. aegypti* Liverpool-IB12 (LVP-IB12) strain was used in these investigations and reared as previously described (Clemons et al., 2010b).

Chitosan/siRNA-nanoparticle mediated KD

KD of *sema1a* was achieved via chitosan/siRNA-nanoparticle feedings. Both the control and siRNAs targeting *sema1a* (siRNA^{890} and siRNA^{1198}) that were utilized in this investigation have been described previously (Haugen et al., 2011) and used for chitosan/siRNA mediated targeting of *sema1a* during the larval and pupal stages (Mysore et al., 2013). Chitosan/siRNA nanoparticles were prepared as described in Mysore et al. (2013) using a protocol that was modified from Zhang et al. (2010). Briefly, *A. aegypti* larvae fed on nanoparticles for four h time periods daily for three days (one pellet/feeding/50 larvae). KD levels, which were quantified through qRT-PCR assays in our previous study in which the same technique was employed at these developmental stages (Mysore et al., 2013), was confirmed here through *in situ* hybridization and antibody staining (see details below). For all specific phenotypes assessed, two or more replicate experiments (n = 50 per control or experimental group) were performed with siRNA^{890}, siRNA^{1198}, and control-fed, or wildtype animals.

Staining and imaging

Immunohistochemical staining was carried out as described earlier (Clemons et al., 2010c; Mysore et al., 2011; Mysore et al., 2013). Briefly, anti-acetylated Tubulin (1:200; Jackson Immunoresearch, West Grove, PA) and anti-HRP conjugated to Cy3 (1:100; Jackson Immunoresearch, West Grove, PA) antibodies were used to view axon trajectories. Rat anti-5HT (1:100; Abcam, Cambridge, MA) was used to mark serotonergic higher order visual neurons. mAb 22C10 (1:20; Fujita et al., 1982; Zipursky et al., 1984) was provided by Nipam H. Patel. Rabbit anti-Sema1a (1:1000; kindly provided by A. Kolodkin) was used to analyze Sema1a protein expression. This antibody (Yu et al., 1998) was generated against an extracellular region of *D. melanogaster* Sema1a that is conserved in *A. aegypti* and is known

to detect *Aae* Sema1a in the developing brain (Mysore et al., 2013). Goat anti-mouse 647, goat anti-rabbit FITC (Jackson Immunoresearch, West Grove, PA), and Alexa Fluor 568 goat anti-rat IgG (Life Technologies, Grand Island, NY) secondary antibodies were used at a concentration of 1:200. Imaging was performed with a Zeiss 710 confocal microscope using Zen software, and scanned images were analyzed using FIJI and Adobe Photoshop software.

For *in situ* hybridization, digoxygenin-labeled antisense and sense control riboprobes were synthesized according to the Patel (1996) protocol for *sema1a (AAEL002653). In situ* hybridization was performed as previously described (Haugen et al., 2010). Samples were imaged on a Zeiss brightfield microscope using a Spot camera and associated software.

Electroretinogram (ERG) analyses

For full-field ERG measurements, mosquitoes were anaesthetized with diethyl ether and immobilized with wax onto a glass cover slip. Two glass electrodes were filled with 0.2 M sodium chloride solution and mounted. The recording electrode was inserted into the retina of the mosquito, while the grounding electrode was inserted through the opposite eye into the brain. While kept in darkness, the mosquito was pulsed with 1 s of light between intervals of darkness. The light source was equipped with neutral density filters, which were used in combination to attenuate the light. Each light pulse increased the intensity of light by one log unit until the last exposure in which no filter was used, i.e. -7, -6, -5, -4, -3, -2, -1, and 0, respectively. Data from recordings were normalized and analyzed using Prism software (Version 5.0).

Larval photoavoidance assay

L4 larvae are negatively phototactic (Christophers, 1960), a response that can be measured in a simple behavioral assay that was performed in the following manner. A 15mm petri dish base was covered with neutral density (ND) filters (SGXND 15, Solar Graphics, FL). The ND filters were cut and stacked one above the other, creating a gradient of darkness ranging from darkest (100% dark) on one side of the dish to lightest (0% dark) on the opposite side (no filter), with increments of 25% increases of lightness between the two sides. This dish was placed on a light box and kept in a darkroom. For each assay, prior to the introduction of light, L4 larvae were placed in the dish and allowed to distribute randomly for 10 min. After this period, 60 s assays were conducted in which the responses of larvae in the group were video recorded following the introduction of light, which occurred at time = 4 s (Fig. 6A). Four groups of 25 larvae each (wildtype, control, siRNA^{890} and siRNA^{1198}) were assayed in each of four replicate experiments. The videos were analyzed following conduction of the assay, at which time the positions of larvae (0%, 25%, 50%, 75%, or 100% darkness) at 1 s intervals were noted. The average amount of times required for the groups of larvae to move to the darkness, the amount of time they spent in the darkness, and the percentage of larvae remaining in the darkness at the end of the 60 s assay were plotted. Data were statistically evaluated with ANOVA (Origin Pro 8).

Accession numbers

A. aegypti sema1a corresponds to Vectorbase AAEL002653 and NCBI Reference Sequence XP_001661952.1.

Acknowledgments

Thanks to members of the lab and the Eck Institute for Global Health for their advice and comments on the manuscript. This work was supported by NIH/NIAID Award R01-AI081795 to MDS. EMF was supported through a Notre Dame Eck Institute for Global Health graduate fellowship.

REFERENCES

Allan SA, Day JF, Edman JD. Visual ecology of biting flies. Annu Rev Entomol. 1987; 32:297–316. [PubMed: 2880551]

Bentley MD, Day JF. Chemical ecology and behavioral aspects of mosquito oviposition. Annu Rev Entomol. 1989; 34:401–421. [PubMed: 2564759]

Bowen MF. The sensory physiology of host-seeking behavior in mosquitoes. Annu Rev Entomol. 1991; 36:139–158. [PubMed: 1672499]

Brown PK, White RH. Rhodopsin of the larval mosquito. J Gen Physiol. 1972; 59:401–414. [PubMed: 5029551]

Buschbeck EK, Friedrich M. Evolution of insect eyes: tales of ancient heritage, deconstruction, reconstruction, remodeling, and recycling. Evo Edu Outreach. 2008; 1:448–462.

Cafferty P, Yu L, Long H, Rao Y. Semaphorin-1a functions as a guidance receptor in the *Drosophila* visual system. J Neurosci. 2006; 26:3999–4003. [PubMed: 16611816]

Christophers, SR.; Aëdes aegypti (L.). The yellow fever mosquito: its life history, bionomics and structure. Cambridge University Press; Cambridge: 1960.

Clemons A, Haugen M, Flannery E, Tomchaney M, Kast K, Jacowski C, Le C, Mori A, Simanton Holland W, Sarro J, Severson DW, Duman-Scheel M. *Aedes aegypti:* an emerging model for vector mosquito development. Cold Spring Harb Protoc. 2010a; 2010 pdb emo141.

Clemons A, Mori A, Haugen M, Severson DW, Duman-Scheel M. Culturing and egg collection of *Aedes aegypti*. Cold Spring Harb Protoc. 2010b; 2010 pdb prot5507.

Clemons A, Flannery E, Kast K, Severson D, Duman-Scheel M. Immunohistochemical analysis of protein expression during *Aedes aegypti* development. Cold Spring Harb Protoc. 2010c; 2010 pdb prot5510.

Flannery E, Duman-Scheel M. Semaphorins at the interface of development and cancer. Curr Drug Targets. 2009; 10:611–619. [PubMed: 19601765]

Friedrich M. Evolution of insect eye development: first insights from fruit fly, grasshopper and flour beetle. Integr Comp Biol. 2003; 43:508–521. [PubMed: 21680459]

Fujita SC, Zipursky SL, Benzer S, Ferrus A, Shotwell SL. Monoclonal antibodies against the *Drosophila* nervous system. Proc Natl Acad Sci USA. 1982; 79:7929–7933. [PubMed: 6818557]

Gilbert C. Form and function of stemmata in larvae of holometabolus insects. Annu Rev Entomol. 1994; 39:323–349.

Grueber WB, Graubard K, Truman JW. Tiling of the body wall by multidendritic sensory neurons in *Manduca sexta*. J Comp Neurol. 2001; 440:271–283. [PubMed: 11745623]

Haugen M, Flannery E, Tomchaney M, Mori A, Behura SK, Severson DW, Duman-Scheel M. Semaphorin-1a is required for *Aedes aegypti* embryonic nerve cord development. PLoS One. 2011; 6:e21694. [PubMed: 21738767]

Haugen M, Tomchaney M, Kast K, Flannery E, Clemons A, Jacowski C, Simanton Holland W, Le C, Severson D, Duman-Scheel M. Whole-mount in situ hybridization for analysis of gene expression during *Aedes aegypti* development. Cold Spring Harb Protoc. 2010; 2010 pdb prot5509.

Megy K, Emrich SJ, Lawson D, Campbell D, Dialynas E, Hughes DS, Koscielny G, Louis C, Maccallum RM, Redmond SN, Sheehan A, Topalis P, Wilson D, VectorBase C. VectorBase: improvements to a bioinformatics resource for invertebrate vector genomics. Nucleic Acids Res. 2012; 40:D729–734. [PubMed: 22135296]

Moses, K. *Drosophila* eye development: results and problems in cell differentiation. Springer-Verlag; Berlin: 2002.

Mysore K, Flister S, Muller P, Rodrigues V, Reichert H. Brain development in the yellow fever mosquito *Aedes aegypti:* a comparative immunocytochemical analysis using cross-reacting

antibodies from *Drosophila melanogaster*. Dev Genes Evol. 2011; 221:281–296. [PubMed: 21956584]

Mysore K, Flannery EM, Tomchaney M, Severson DW, Duman-Scheel M. Disruption of *Aedes aegypti* olfactory system development through chitosan/siRNA nanoparticle targeting of semaphorin-1a. PLoS Negl Trop Dis. 2013; 7:e2215. [PubMed: 23696908]

Mysore K, Andrews E, Li P, Duman-Scheel M. Chitosan/siRNA nanoparticle targeting demonstrates a requirement for single-minded during larval and pupal olfactory system development of the vector mosquito *Aedes aegypti*. BMC Dev Bio. 2014; 14:9. [PubMed: 24552425]

Patel, N. In situ hybridization to whole mount *Drosophila* embryos. Krieg, PA., editor. Wiley-Liss; New York: 1996. p. 357-370.

Paulk A, Millard SS, van Swinderen B. Vision in *Drosophila:* seeing the world through a model's eyes. Annu Rev Entomol. 2013; 58:313–332. [PubMed: 23020621]

Pecot M, Tadros W, Nern A, Bader M, Chen Y, Zipursky L. Multiple interactions control synaptic layer specificity in the *Drosophila* visual system. Neuron. 2013; 77:299–310. [PubMed: 23352166]

Seldin EB, White RH, Brown PK. Spectral sensitivity of larval mosquito ocelli. J Gen Physiol. 1972; 59:415–420. [PubMed: 5029552]

Steven DM. The dermal light sense. Biol Rev Camb Philos Soc. 1963; 38:204–240. [PubMed: 4385905]

Toh Y, Mizutani A. Visual-system of the tiger beetle *(Cicindela chinensis)* larva. 1. Structure. Zoolog Sci. 1987; 4:974.

White RH. Analysis of the development of the compound eye in the mosquito, *Aedes aegypti*. J Exp Zool. 1961; 148:223–239. [PubMed: 14006559]

Winberg ML, Noordermeer JN, Tamagnone L, Comoglio PM, Spriggs MK, Tessier-Lavigne M, Goodman CS. Plexin A is a neuronal semaphorin receptor that controls axon guidance. Cell. 1998; 95:903–916. [PubMed: 9875845]

Wolff, T.; Ready, DF. Pattern formation in the *Drosophila* retina. Bate, M.; Martinez Arias, A., editors. Cold Spring Harbor Press; New York: 1993. p. 1277-1325.

Xiang Y, Yuan Q, Vogt N, Looger LL, Jan LY, Jan YN. Light-avoidance-mediating photoreceptors tile the *Drosophila* larval body wall. Nature. 2010; 468:921–926. [PubMed: 21068723]

Yu HH, Araj HH, Ralls SA, Kolodkin AL. The transmembrane semaphorin sema I is required in *Drosophila* for embryonic motor and CNS axon guidance. Neuron. 1998; 20:207–220. [PubMed: 9491983]

Yu L, Zhou Y, Cheng S, Rao Y. Plexin A-semaphorin-1a reverse signaling regulates photoreceptor axon guidance in *Drosophila*. J Neurosci. 2010; 30:12151–12156. [PubMed: 20826677]

Zhang X, Zhang J, Zhu KY. Chitosan/double-stranded RNA nanoparticle-mediated RNA interference to silence chitin synthase genes through larval feeding in the African malaria mosquito *(Anopheles gambiae)*. Insect Mol Biol. 2010; 19:683–693. [PubMed: 20629775]

Zipursky SL, Venkatesh TR, Teplow DB, Benzer S. Neuronal development in the *Drosophila* retina: monoclonal antibodies as molecular probes. Cell. 1984; 36:15–26. [PubMed: 6420071]

Key Findings

- The progression of post-embryonic visual system development was characterized in the dengue vector mosquito *Aedes aegypti*.
- Sema1a is required for establishment of a retinotopic map during *Aedes aegypti* optic lobe development.
- Loss of *sema1a* results in larval photoavoidance behavioral defects.

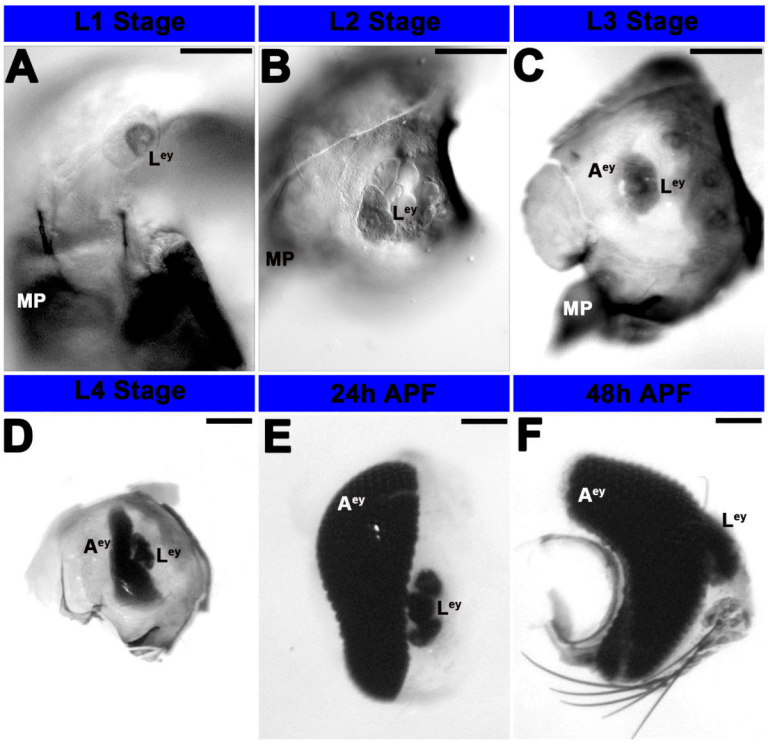

Figure 1. Development of the eye in *A. aegypti*

Progressive development of the eye from L1 larvae (A) to 48h APF (F) was visualized through differential interference contrast (DIC) optics (A-F). L1 (A) and L2 (B) larvae possess fairly simple larval eyes (L^{ey}) that are visible at least through 48 h APF; it is unclear if these persist in adults. By stage L3, the adult eye is also visible (C), and it is noticeably larger in L4 animals (D). By the pupal stage (24 h APF in E, 48 h APF in F), additional rows of differentiated photoreceptor cells are visible in the adult eye, which has become a complex primary visual center. Scale bar = 25 microns; L^{ey}: larval eye; A^{ey}: adult eye; MP: mouth parts. Dorsal is oriented upward in all panels.

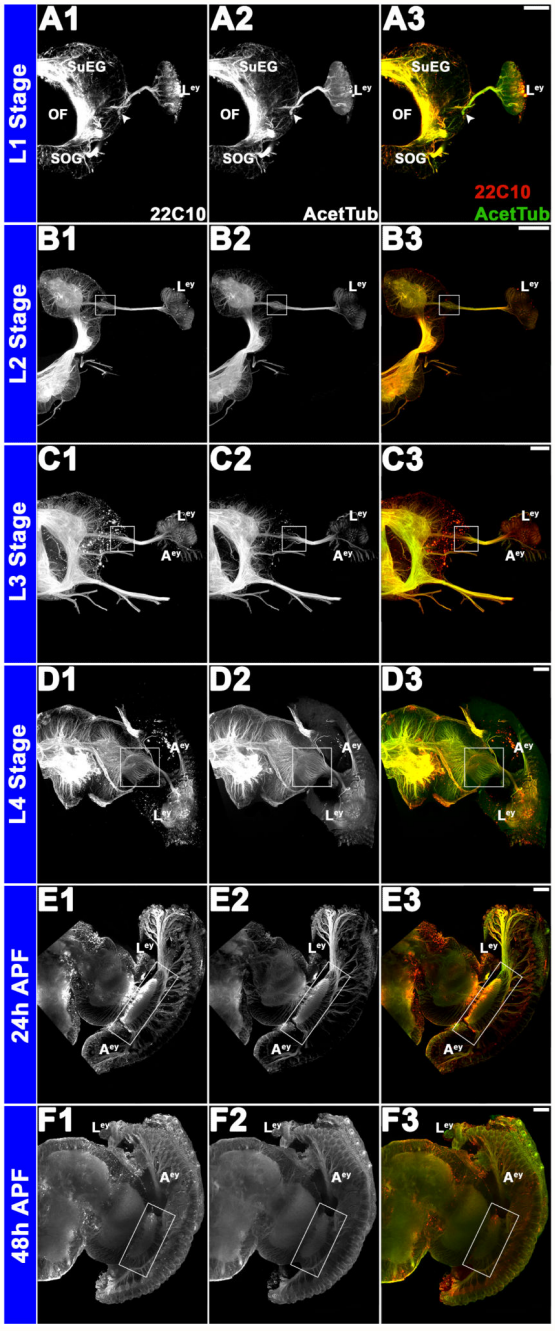

Figure 2. Structure and development of the visual system in *A. aegypti*

Progressive development of the larval and adult eyes and corresponding development of the brain was visualized from L1 (A1-A3) to 48 h APF (F1-F3) through immunolabeling with mAb 22C10 (A1-F1; red in overlays at right) and anti-acetylated Tubulin (A2-F2; green in overlays at right). White arrowheads in A1-A3 and white boxes in subsequent panels mark the primary visual center, which becomes progressively more complex during the larval (L1 in A1-A3; L2 in B1-B3; L3 in C1-C3; L4 in D1-D3) and pupal (24 h APF in E1-E3; 48 h APF in F1-F3) stages. Labeling with the visual sensory neuron marker 22C10 (A1-F1) co-

localizes with anti-acetylated tubulin antibody staining (A2-F2), which is used to label the visual sensory neurons in subsequent figures. Scale bar = 25 microns; A^{ey}: adult eye; OF: esophageous foramen; L^{ey}: larval Eye; MP: mouth parts; SOG: subesophageal ganglion; SuEG: supraesophageal ganglion. Dorsal is oriented upward in all panels.

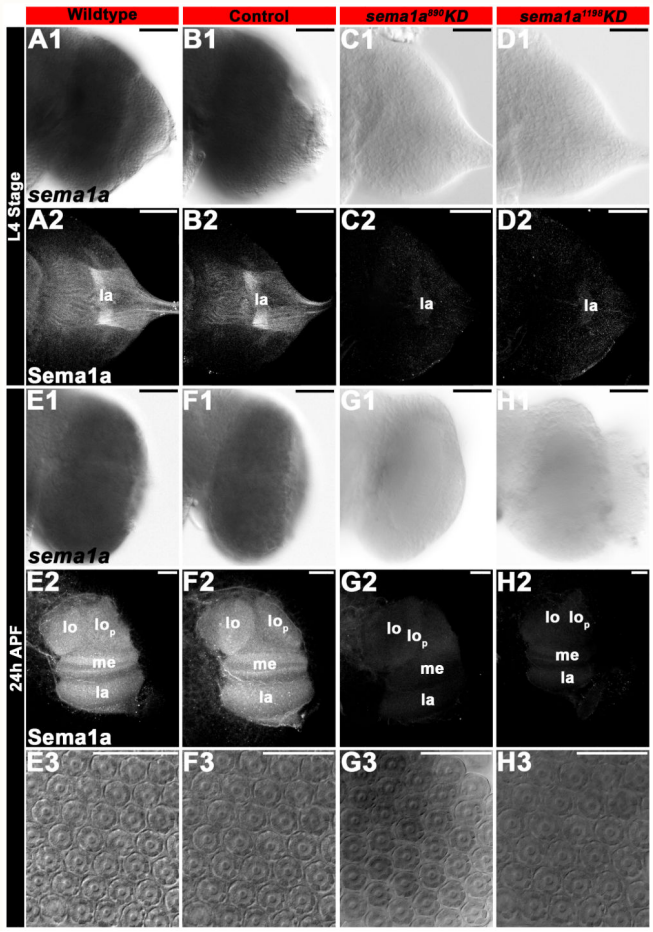

Figure 3. siRNA-mediated KD of *sema1a* in the *A. aegypti* developing visual system

sema1a mRNA (A1, B1, E1, F1) and protein (A2, B2, E2, F2) expression is detected in the developing L4 larval (A1, B1, A2, B2) and 24 h APF pupal (E1, F1, E2, F2) optic lobes of wildtype (A1, A2, E1, E2) and control-fed (B1, B2, F1, F2) animals. *sema1a* siRNA^{890} (C1, C2, G1, G2) and siRNA^{1198} (D1, D2, H1, H2) effectively KD expression of *sema1a* transcript in developing *A. aegypti* L4 larvae (C1, D1 vs. A1, B1) and 24 h APF pupae (G1, H1 vs. E1, F1). KD was also confirmed through examination of Sema1a protein expression in the developing optic lobes of L4 larvae (C2, D2 vs. A2, B2) and 24 h APF pupae (G2, H2 vs. E2, F2). The optic lobe of one brain hemisegment oriented dorsal upward is shown in all panels except E3-H3, in which DIC images of 24 h APF pupal ommatidial clusters in wildtype (E3), control-fed (F3) and *sema1a* KD animals (siRNA^{890} in G3 and siRNA^{1198} in H3) are shown. Scale bar = 25 microns; lo: lobula; lo^{p}: lobula plate; me: medulla; la: lamina.

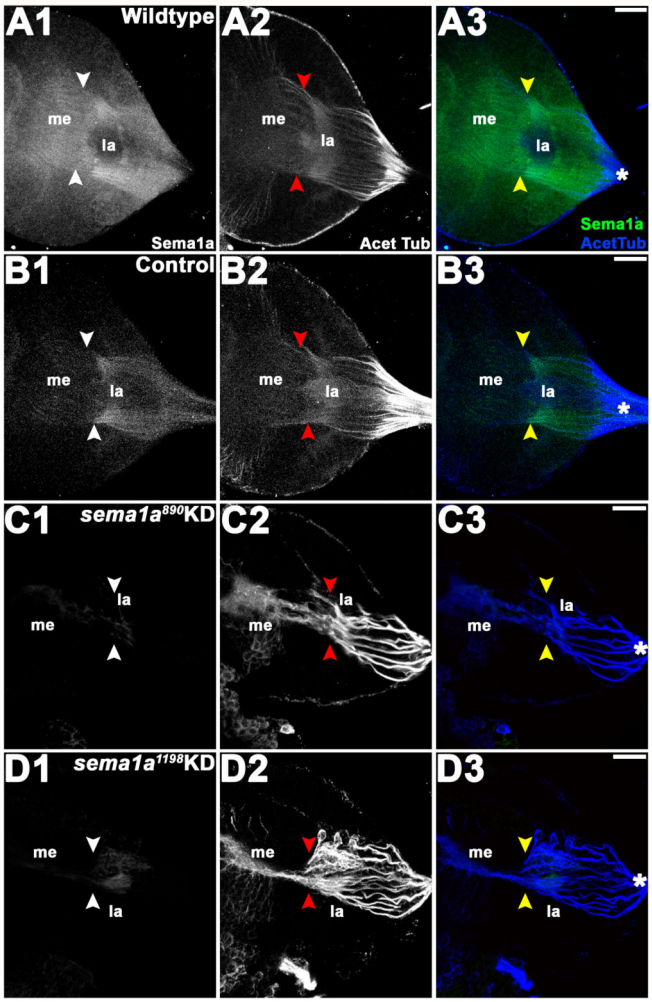

Figure 4. Visual sensory neuron targeting defects in *sema1a* KD larvae

In wildtype (A1-A3) and control-fed (B1-B3) larvae, the visual sensory neurons labeled by anti-acetylated Tubulin antibody staining (A2, B2), which enter the optic lobe of the brain as a bundle (asterisks in A3, B3), sort at the lamina (la), where a dense terminal layer forms. From the lamina, a subset of visual sensory axons proceed toward the medulla (me) as individual tracts with specific patterns (white/red/yellow arrowheads). In individuals fed with *sema1a* siRNA (siRNA^{890} in C1-C3, siRNA^{1198} in D1-D3), visual sensory neurons (C2, D2) enter the brain through the optic lobe normally (asterisks), but the terminal layer does not form properly in the lamina. Many of the visual sensory neurons extend together beyond the lamina toward the medulla, where they fail to target appropriately as individual tracts. The targeting defects observed in visual sensory neurons correlate with a significant decrease in the expression of Sema1a as revealed by anti-Sema1a antibody staining (C1, D1 vs. A1, B1). Overlays of both labels (Sema1a in green and acetylated Tubulin in blue) are shown in A3-D3. The optic lobe of one brain hemisegment oriented dorsal upward is shown in all panels. Scale bar = 25 microns.

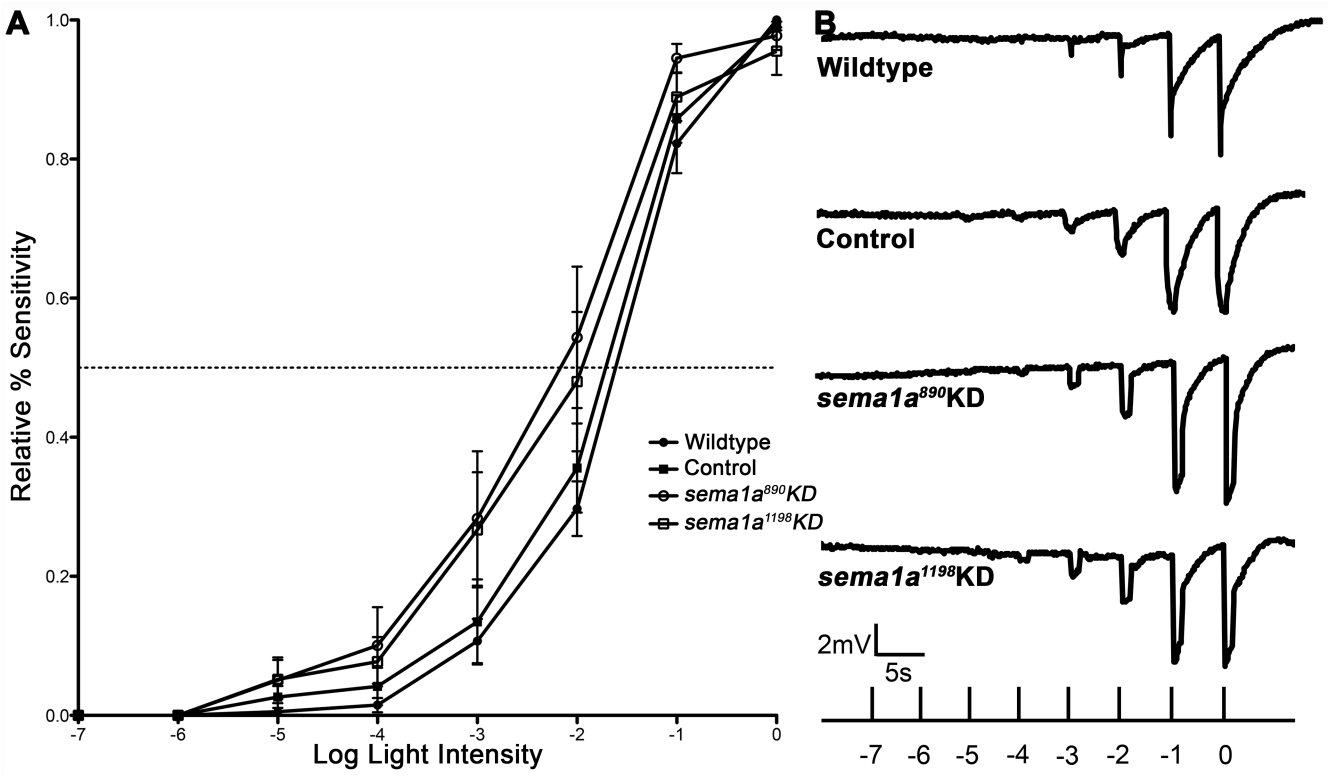

Figure 5. *sema1a* loss of function photoreceptor cells are light-sensitive

(A) No differences in light sensitivity were detected through full-field ERG analyses in wildtype adults vs. adults fed with control, *sema1a* KD siRNA^{890}, or siRNA^{1198} as larvae. The numbers of individuals recorded for each treatment were: wildtype=7; control=9; *sema1a* KD *siRNA*^{890}=7; *sema1a* KD siRNA^{1198}=8. Error bars represent standard errors of the means (SEMs). (B) Representative traces from a wildtype animal and the indicated control or *sema1a* KD siRNA-fed animals are shown.

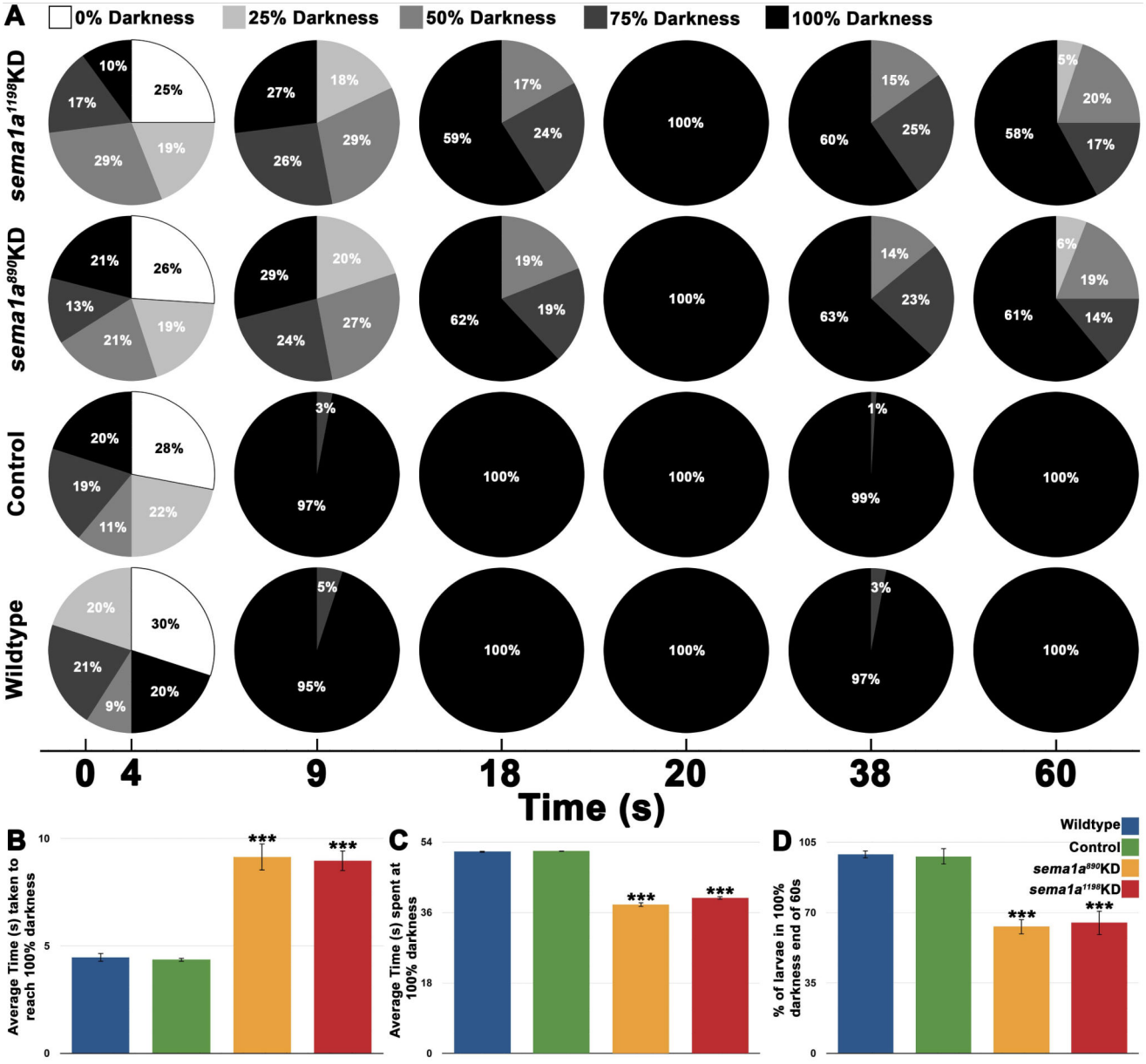

Figure 6. *sema1a* KD larvae behave abnormally in a larval photoavoidance assay

Light was differentially blocked by filters to achieve zones of differential darkness, ranging from 0 – 100% darkness in 25% intervals. The % darkness zonal locations of 25 larvae for each experimental condition (wildtype, control-fed, siRNA^{890}, and siRNA^{1198}) was measured at 1 s intervals during a 60 s assay during each of four replicate experiments. The pie charts in A represent the combined totals for each experimental condition from the four replicate experiments at 0, 4, 9, 18, 20, 38, and 60 s. The pie charts at t = 4 s depict the initial random distribution of larvae kept in 100% darkness prior to light introduction, which occurred at this time point (A). Wildtype and control-fed L4 larvae are negatively phototactic and swam to 100% darkness within 5 s of light introduction (A). Once they reached 100% darkness, wildtype and control-fed animals remained in the 100% darkness

zone for the duration of the 60 s assay (A). No significant differences were detected between wildtype and control-fed animals in these assays (B-D). *sema1a* KD L4 larvae fed with siRNA^{890} or siRNA^{1198} also moved to 100% darkness (A), but at a significantly slower rate in comparison to wildtype or control fed-animals ($p<0.001$; B), and remained in the darkness for a significantly shorter period of time ($p<0.001$; C). At the end of the assay, a significantly lower percentage of KD larvae were found in 100% darkness ($p<0.001$; D). No significant differences were detected between siRNA^{890} and siRNA^{1198}-fed animals in these assays (B-D). Asterisks (***) denote significant differences ($p<0.001$) between *sema1a* KD groups vs. both wildtype and control-fed groups. Error bars represent SEMs.

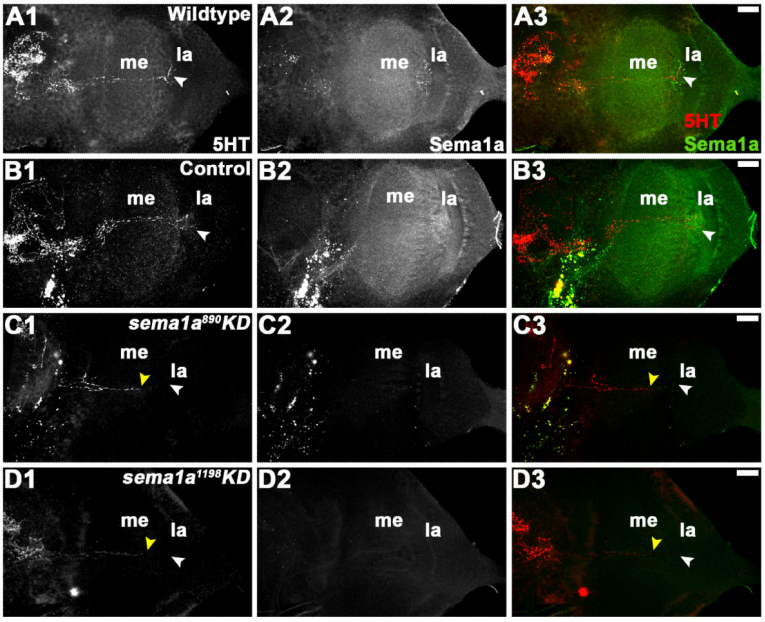

Figure 7. ***sema1a*** **KD results in disruption of higher order visual neuron projections in the larval optic lobe**

In wildtype (A1-A3) and control-fed (B1-B3) L4 larval brains, 5HT-positive higher order neurons terminate in the lamina (la; white arrowhead in A1, B1). In comparably staged L4 individuals fed with siRNA^{890} (C1-C3) or siRNA^{1198} (D1-D3), the projections of 5HT-positive neurons terminate (yellow arrowhead in C1, D1) prior to reaching their laminar target (white arrowhead in C1, D1). These individuals lack expression of Sema1a (C2, D2 vs. A2, B2). Overlays of both labels are shown in A3-D3 (5HT in red; Sema1a in green). The optic lobe of one brain hemisegment oriented dorsal upward is shown in all panels. Scale bar = 25 microns; me: medulla; la: lamina.

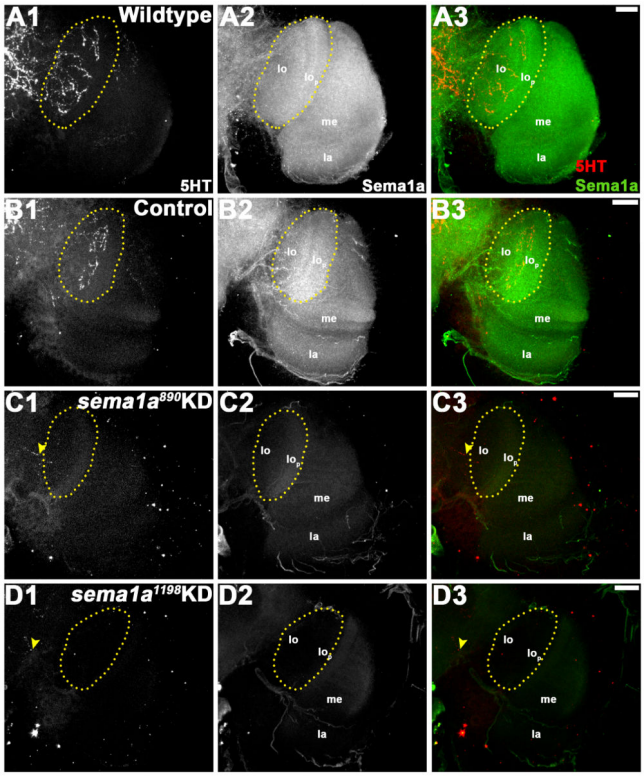

Figure 8. Higher order visual neurons in the optic lobe fail to reach their targets in *sema1a* KD pupae

24 h APF wildtype (A1-A3) and control-fed (B1-B3) pupae were labeled with anti-5HT antibody staining, which revealed higher order neural defects in the optic lobe (A1, B1). Similar to larval 5HT neurons, these neurons project from the supraoesophageal ganglion and terminate with a thick arborization in the lobula (lo) region of the optic lobe (highlighted by yellow dots in A1, B1). In comparably staged *sema1a* KD animals fed with siRNA^{890} (C1-C3) or siRNA^{1198} (D1-D3), the 5HT neurons terminate without entering the optic lobe (yellow arrow head in C1, D1). This phenotype correlated with a lack of Sema1a expression in these individuals (Sema1a antibody staining in C2, D2 vs. A2, B2). Overlays of both labels are shown in A3-D3 (5HT in red; Sema1a in green). The optic lobe of one brain hemisegment oriented dorsal upward is shown in all panels. Scale bar = 25 microns; lo: lobula; lo^{p}: lobula plate; me: medulla; la: lamina.

Table 1

Assessment of siRNA-mediated *sema1a* KD. The set of data represents a compiled summary of results obtained from four replicate experiments in which *sema1a* transcript (top) or protein (bottom) levels were assessed through whole mount *in situ* hybridization (as in Fig. 3) or immunohistochemistry (as in Figs. 4, 7, 8) in control-fed vs. *sema1a* KD animals. The number of optic lobes assessed (n) in L4 larvae (left) or 24 h pupae (right) and the percentages of optic lobes with normal (compared to wildtype) or reduced (less than wildtype) *sema1a* transcript or Sema1a protein expression levels are indicated.

	LARVAL OPTIC LOBE			PUPAL OPTIC LOBE		
siRNA	**n**	**% Normal**	**% Reduced**	**n**	**% Normal**	**% Reduced**
	Analysis of KD through in situ hybridization with sema1a probe					
Control-fed	50	100	0	50	100	0
sema1a^{890}KD	50	28	72	50	36	64
sema1a^{1198}KD	50	32	68	50	36	64
	Analysis of KD through Sema1a protein labeling					
Control-fed	50	100	0	50	100	0
sema1a^{890}KD	50	40	60	50	50	50
sema1a^{1198}KD	50	36	64	50	45	55

Table 2

The set of data represents a compiled summary of results obtained for control-fed vs. *sema1a* knockdown (KD) animals from a total of four replicate experiments performed in L4 larvae (left, middle) and 24 h pupae (right). The total number of optic lobes (OL) assessed (n) and percentages of animals displaying wildtype (WT) morphology, L4 visual sensory neuron targeting defects, L4 or 24 h pupal optic lobe serotonergic neuron targeting defects are indicated. Knockdown was immunohistochemically confirmed through anti-Sema1a antibody staining.

	L4 Visual Sensory Neuron Targeting			L4 OL Serotonergic Neuron Targeting			Pupal OL Serotonergic Neuron Targeting		
siRNA	**n**	**% WT**	**% Defective**	**n**	**% WT**	**% Defective**	**n**	**% WT**	**% Defective**
Control-fed	90	100	0	50	100	0	50	100	0
sema1a^{890}KD	90	40	60	50	40	60	50	44	56
sema1a^{1198}KD	90	38	62	50	40	60	50	48	52